Nuclear Engineering and Technology 52 (2020) 1148–1155

Contents lists available at ScienceDirect

Nuclear Engineering and Technology

journal homepage: www.elsevier.com/locate/net

Original Article

On using computational versus data-driven methods for uncertainty propagation of isotopic uncertainties

Majdi I. Radaideh*, Dean Price, Tomasz Kozlowski

Department of Nuclear, Plasma, and Radiological Engineering, University of Illinois at Urbana Champaign, Urbana, IL, 61801, USA

ARTICLE INFO

Article history:
Received 8 October 2019
Received in revised form
1 November 2019
Accepted 25 November 2019
Available online 25 November 2019

Keywords:
Isotopic composition
Radiochemcial assay data
Uncertainty quantification
SCALE/KENO-V.a
Criticality safety
SFCOMPO

ABSTRACT

This work presents two different methods for quantifying and propagating the uncertainty associated with fuel composition at end of life for cask criticality calculations. The first approach, the computational approach uses parametric uncertainty including those associated with nuclear data, fuel geometry, material composition, and plant operation to perform forward depletion on Monte-Carlo sampled inputs. These uncertainties are based on experimental and prior experience in criticality safety. The second approach, the data-driven approach relies on using radiochemcial assay data to derive code bias information. The code bias data is used to perturb the isotopic inventory in the data-driven approach. For both approaches, the uncertainty in k_{eff} for the cask is propagated by performing forward criticality calculations on sampled inputs using the distributions obtained from each approach. It is found that the data driven approach yielded a higher uncertainty than the computational approach by about 500 pcm. An exploration is also done to see if considering correlation between isotopes at end of life affects k_{eff} uncertainty, and the results demonstrate an effect of about 100 pcm.

1. Introduction

In nuclear criticality safety, uncertainty could originate from nuclear data libraries, fuel depletion calculations, isotopic inventory, and cask design [1]. Propagation of nuclear data uncertainties into criticality safety applications is a well-understood topic, as adjoint-based and sampling-based methods were thoroughly used to quantify the uncertainty in cask k_{eff}. However, the effect of the uncertainty in the isotopic inventory needs more attention, especially because the nuclide composition plays a major role in determining cask criticality.

One study [2] explored the effect of nuclear data uncertainties on various PWR operating parameters like reactivity swing, isotopic inventory, and radiotoxicity. A Monte Carlo approach was used, similar in concept to the computational approach presented in this study. Nuclear data pertaining to U-235, U-236, U-238, and Pu-239 were varied both independently and together. It was found that U-236 has a negligible impact on the quantities explored in this study. Another study was conducted for a spent fuel pool [3]. A tool named MTUQ was used in this study, where manufacturing and technological parameter tolerances (e.g. pellet radius, clad density) were considered in the uncertainty analysis. It was found that the main contributors to the total variance in k_{eff} are related to the storage rack components such as absorber box inner width. A minor part of Ref. [4] used stochastic sampling methods to propagate uncertainty through a pin cell model using the multiphysics code VERA. Two methods, one incorporating a sensitivity analysis and another one performed by global random sampling, were used that yielded similar results. A study [5] investigated alternatives to a conventional "5%" uncertainty approach using statistical methods similar to the previous papers. Lastly, criticality safety analysis under assembly misloading has been conducted by Ref. [6], which incorporated adjoint-based sensitivity and uncertainty analyses.

As majority of previous efforts focused on nuclear data uncertainties as a major part of criticality safety uncertainties, this work highlights uncertainty quantification (UQ) of the isotopic uncertainty. In this paper, uncertainty in the spent fuel composition at the end of life will be investigated and quantified using two different approaches. The first approach is a computational approach and involves sampling from input parameter distributions and performing forward calculations on these sampled cases. This creates uncertainties in the nuclide inventory. The input uncertainties for this approach include assembly geometry, nuclear data, material parameters, and operating conditions. Although this

* Corresponding author.
E-mail address: radaide2@illinois.edu (M.I. Radaideh).

https://doi.org/10.1016/j.net.2019.11.029

approach still relies on data that comes from experiments (e.g. nuclear data) or prior experience (e.g. fuel design), it is called computational in this work since the initial input uncertainties are propagated purely based on the computational model without intervention from experimental data after depletion. On the other hand, the second approach is a data-driven approach which uses nuclide experimental data derived from radiochemical assay experiments to create bias information (C/E) which represents the calculated to measured difference. Therefore, no Monte Carlo sampling is performed during depletion calculations for the second approach. The bias for each nuclide is then randomly sampled and used as a perturbation factor for the nominal nuclide inventory obtained from depletion calculations. The perturbed nuclide inventory is then propagated through cask calculations. The two approaches are demonstrated using BWR GE10x10 lattice model and GBC-68 spent fuel cask, and conclusions about their results are drawn.

2. UQ Methodology

This section is organized into three subsections. The first subsection describes a general sampling approach that will be described once and used multiple times throughout this work. The second subsection is concerned with quantifying isotopic uncertainty in the fuel at the end of cycle. This is done with two different approaches, a computational approach and a data-driven approach, each will be explained in detail. The third subsection outlines how the uncertainties in fuel composition, calculated in the previous subsection, are carried through cask criticality calculations to get final cask k_{eff} with uncertainty.

2.1. Normal distribution statistics with physical models

Overall, the normal distribution will be used mainly to sample the input vectors in this study, whether these inputs are correlated (multivariate) or independent (univariate). After applying a physical model (i.e. depletion or criticality) to the input vector, an output vector is obtained. If the physical model is applied on random/sampled input vectors, the corresponding output vectors can be computed for each sampled input. Mathematically, all d input parameters (X_j, $j = 1, \ldots, d$) are sampled from their d-dimensional joint/marginal normal distribution

$$\boldsymbol{X}^{(i)} \sim \mathcal{N}_d(\boldsymbol{\mu}, \boldsymbol{\Sigma}), \quad i = 1, \ldots, N, \tag{1}$$

where N indicates the number of vectors sampled in the input space, $\boldsymbol{\mu} = (\mathrm{E}[X_1], \mathrm{E}[X_2], \ldots, \mathrm{E}[X_d])$ is the mean vector, and $\boldsymbol{\Sigma} = \mathrm{Cov}[X_i, X_j]$ is the covariance matrix. The mean vector represents the location parameter where samples are most likely to be generated (i.e. similar to the peak of the univariate normal distribution but in multidimensional form). The covariance matrix indicates the level to which two input parameters vary together, and it must be positive semidefinite to be able to draw samples based on Eq. (1) [7]. In cases that do not consider correlation between input parameters, $\boldsymbol{\Sigma}$ becomes a diagonal matrix with the variance of each parameter along the diagonal. Next, the model F is applied to N input vectors to yield N output vectors, each referred to as $\boldsymbol{Y}$

$$\boldsymbol{Y}^{(i)} = F\left(\boldsymbol{X}^{(i)}\right), \quad i = 1, \ldots, N. \tag{2}$$

Following this process, two statistical moments can be used to characterize the output. In the case of multiple outputs, the mean and covariance matrix can be calculated as follows

$$\overline{\boldsymbol{Y}} = \frac{1}{N}\sum_{i=1}^{N} \boldsymbol{Y}^{(i)}, \tag{3}$$

$$\boldsymbol{\Sigma}_{\boldsymbol{Y}} = \mathrm{E}\left[(\boldsymbol{Y} - \overline{\boldsymbol{Y}})(\boldsymbol{Y} - \overline{\boldsymbol{Y}})^T\right]. \tag{4}$$

In the case of single output, as is the case in criticality calculations (i.e. k_{eff}), the above equations reduce to a simple scalar mean and variance, given below

$$\overline{Y} = \frac{1}{N}\sum_{i=1}^{N} Y^{(i)}, \tag{5}$$

$$\sigma_Y^2 = \frac{1}{N}\sum_{i=1}^{N} \left(Y^{(i)} - \overline{Y}\right)^2. \tag{6}$$

2.2. Depletion UQ

In this section, two different methods of identifying uncertainties in isotopic composition at end of life are used. The computational approach performs forward depletion calculations on the lattice model that will be loaded into the cask for criticality calculations. The data-driven model uses pre-determined code bias data to determine the isotopic uncertainty at the end of cycle.

2.2.1. Computational approach

As mentioned earlier, two separate methods for calculating the uncertainty in the fuel composition at the end of life are used. The first method is the computational approach. In this approach, the process described in Section 2.1 is applied to the depletion models. In this application, $\boldsymbol{X}^{(i)}$ for $i = 1, .., N_b$ is comprised of two groups of input parameters: (1) parameters pertaining to lattice characteristics (geometry, material, operating) and (2) nuclear data parameters used by the depletion code. Also, notice that $N = N_b$, where N_b is the number of random samples for burnup/depletion calculations. For lattice parameters, the method described in Eq. (1) is used with parameters from Table 1 without correlation. For nuclear data, the samples were already generated using a correlated multivariate normal distribution with covariance data available in the SCALE data directory.

These input distributions are applied to a GE10x10 lattice

Table 1
Selected input parameters' uncertainty for lattice depletion calculations (for the computational approach).

Parameter	1-σ (%)	Source
Geometry		
Pellet radius	0.14%	[18,19]
Clad Inner Diameter	0.43%	[18,19]
Clad Outer Diameter	0.46%	[18,19]
Material		
U-235 wt%	0.60%	[14]
Gd_2O_3 wt%	1.67%	[14]
UO_2 Density	0.13%	[18,19]
Operating		
Specific Power	1.67%	[15,16]
Coolant Density	3.33%	[15,16]
Fuel Temperature	3.33%	[15,16]
Nuclear Data		
Neutron Cross-sections	56group-COV	[17]
Fission Yield	56group-COV	[17]
Decay Data	56group-COV	[17]

depletion model described later in Section 3.1. After performing N_b depletion calculations on all $\boldsymbol{X}^{(i)}$, the isotopic composition or concentration of the fuel for sample i can be represented according to Eq. (2), where $\boldsymbol{Y}^{(i)} = \boldsymbol{C}^{(i)}$. Each entry of $\boldsymbol{C}^{(i)}$ represents the isotopic concentration for a particular isotope. The statistics of the output space can then be characterized using Eq. (3) and Eq. (4). Both $\overline{\boldsymbol{C}}$ and $\boldsymbol{\Sigma_C}$ from this analysis will be directly used in Section 2.3 for cask criticality calculations. The summary of the computational approach is presented by the flowchart in Fig. 1.

2.2.2. Data-driven approach

The concept of using experimental data to infer uncertainty bounds was introduced first in Ref. [8] and then applied to PWR [9] and BWR [10] spent fuel analysis. This approach compared to the approach presented in the previous section forgoes performing a large volume of depletion calculations by using external verification data that characterizes the code bias, mis-prediction, or error. The code bias, given in Table 2, is comprised of a distribution of scaling factors that describe the scale and spread of C/E, the ratio of the computed value to the experimental value when replicating fuel assay data. A description of the source of this data is given in Section 3.3. To explain the origin of this data, let us define the ratio between the calculated (C) and experimental (E) values for nuclide n as follows

$$R_n^{(i)} = \frac{C_n^{(i)}}{E_n^{(i)}}, \quad i = 1, \ldots, N_n, \quad n = 1, \ldots, 10, \tag{7}$$

Table 2
The value of bias mean ($\overline{R}_n$) and standard deviation (σ_{R_n}) derived from fuel assay data [21] (for the data-driven approach).

Nuclide	Geometry	$\overline{R}_n$	σ_{R_n}	N_n [a]
U-234	8x8, 7x7	1.0334	0.0416	20
U-235	8x8, 7x7, 6x6	0.9950	0.0539	32
U-236	8x8, 7x7, 6x6	0.9796	0.0205	32
U-238	8x8, 7x7, 6x6	0.9988	0.0048	32
Pu-238	8x8, 7x7, 6x6	0.9505	0.0873	32
Pu-239	8x8, 7x7, 6x6	1.0121	0.0450	32
Pu-240	8x8, 7x7, 6x6	0.9997	0.0349	32
Pu-241	8x8, 7x7, 6x6	0.9876	0.0548	32
Pu-242	8x8, 7x7, 6x6	1.0118	0.0618	32
Am-241	8x8, 7x7	1.0868	0.1208	20

[a] Number of experimental samples available in the 3 benchmarks.

where $E_n^{(i)}$ is the measured value of the nuclide n concentration in the **experimental** sample i, and $C_n^{(i)}$ is the calculated (e.g. code predicted) value of the nuclide n concentration in sample i, N_n is the number of experimental samples available for nuclide n. A total of $n = 10$ actinides is considered in this work. By applying Eq. (5) and Eq. (6), the bias mean ($\overline{R}_n$) and bias uncertainty (σ_{R_n}) can be determined for each nuclide n, respectively.

The data-driven approach requires a special step using the lattice model (GE10x10) to calculate the nominal concentration ($\boldsymbol{C^o}$) of all nuclides. This step is shown in the top section of Fig. 2. Now, given the mean scaling parameter ($\overline{R}_n$) and the nominal concentration (C_n^o) for nuclide n, the vectorized form of the isotopic concentration can be determined with element-wise multiplication of

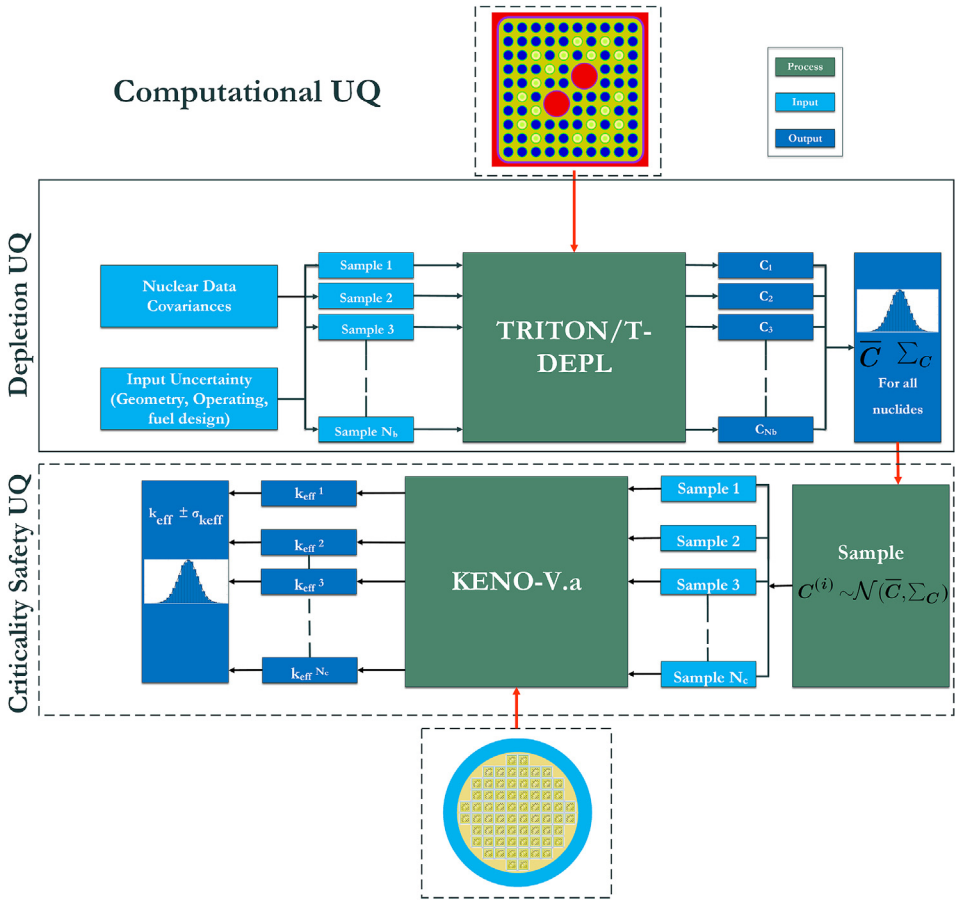

Fig. 1. Flowchart of the computational approach.

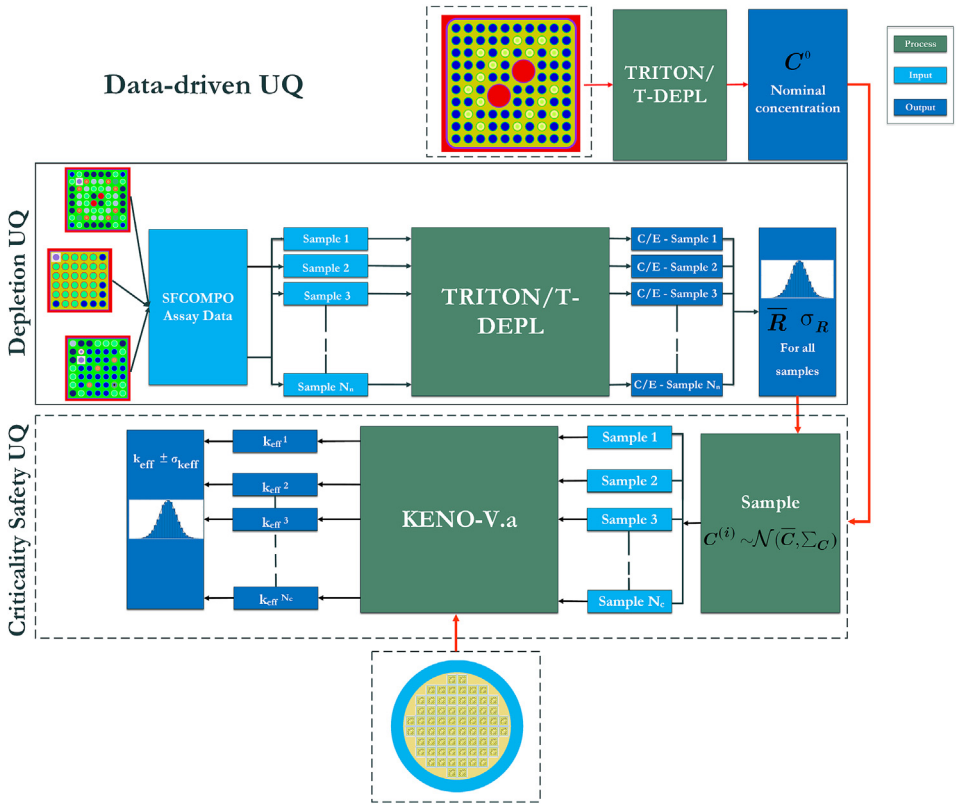

Fig. 2. Flowchart of the data-driven approach.

these two quantities for all isotopes as follows

$$\overline{\boldsymbol{C}} = \left[\overline{R}_1 C_1^o, \overline{R}_2 C_2^o, \cdots, \overline{R}_{10} C_{10}^o\right]. \tag{8}$$

Because of the lack of measurement correlation data, the data-driven approach does not capture the correlation between the isotopic concentrations in this study. This is because the measurement correlation is not reported or assessed during the experiments. As such, the resulting covariance matrix $\boldsymbol{\Sigma_C}$ contains only the variance of each isotopic concentration along the diagonal. The diagonal covariance matrix can be computed with the scaling factor variance $\sigma^2_{\overline{R}_n}$ and the nominal concentration as follows

$$\boldsymbol{\Sigma_C} = \begin{bmatrix} \sigma^2_{\overline{R}_1} C_1^{o2} & & & 0 \\ & \sigma^2_{\overline{R}_2} C_2^{o2} & & \\ & & \ddots & \\ 0 & & & \sigma^2_{\overline{R}_{10}} C_{10}^{o2} \end{bmatrix}. \tag{9}$$

From a physical perspective, $\overline{\boldsymbol{C}}$ represents the mean of the isotopic concentrations after being scaled by the code bias mean, while $\boldsymbol{\Sigma_C}$ expresses the variability in predicting the isotopic concentrations according to the code bias uncertainty. The data-driven approach is summarized in the flowchart in Fig. 2.

2.3. Criticality safety UQ

The next phase in this exploration is the criticality safety UQ, which is shown in Figs. 1–2. The method for operating on the isotopic distributions ($\overline{\boldsymbol{C}}$, $\boldsymbol{\Sigma_C}$) based on each the computational approach and the data-driven approach is the same. An important distinction, is in the computational approach, the covariance matrix contains information on the correlation between isotopes. Since the correlation between experimental samples is not reported for the data-driven approach, the covariance matrix in this case is diagonal.

First, an input vector of isotopic concentrations for the cask criticality calculations can be sampled according to Eq. (1), where $\boldsymbol{\mu} = \overline{\boldsymbol{C}}$ and $\boldsymbol{\Sigma} = \boldsymbol{\Sigma_C}$. Then, a cask criticality calculation for each of the input samples is performed using a criticality code (e.g. KENO-V.a). The relevant result from these calculations is the k_{eff} of the cask. Being scalar, Eq. (5) and Eq. (6) can be used to analyze the final k_{eff} mean and variance.

3. Models and data

3.1. Test models

Two types of test models are needed to demonstrate the two UQ methods: (1) lattice model for depletion calculations inside the core and (2) cask model for criticality calculations. The lattice geometry selected is the GE10x10 lattice. The lattice features 74 UO_2 rods and 18 gadolinium rods with two large water rods replacing 8 fuel rod locations. The original design for the lattice has 7 different UO_2 fuel types and 4 gadolinium pin types with different combinations of U-235 enrichment and gadolinium concentration. To simplify the depletion calculations, the U-235 enrichment and gadolinium concentration are averaged to create two pin types (pins with pure UO_2 and pins with UO_2 and Gd_2O_3) as shown in Fig. 3(a). It has been demonstrated that enrichment averaging radially has a small effect on the depletion trend for this specific lattice design in Ref. [11]. In this work, the lattice is depleted in 2D using the TRITON/T-DEPL sequence in the SCALE code system with reflective boundary conditions. Additional details about the lattice

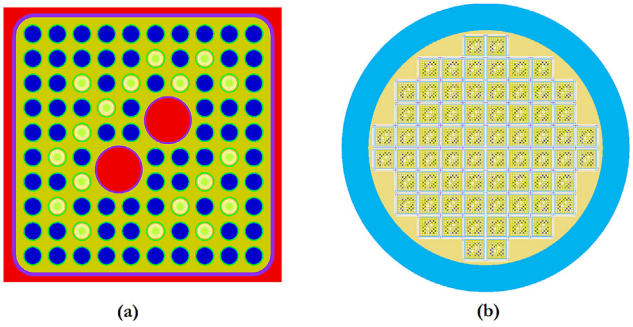

Fig. 3. Schematic representation of: (a) GE10x10 lattice as modeled by TRITON/T-DEPL and (b) GBC-68 spent fuel cask as modeled by KENO-V.a.

design can be found in Refs. [6,12].

The BWR generic burnup credit cask (GBC-68) is selected for criticality calculations, where the isotopic compositions obtained from depletion calculations in TRITON/T-DEPL are loaded into the cask. All 68 spent fuel assemblies are assumed to have identical spent fuel composition (i.e. burnup) as calculated by TRITON/T-DEPL. The cask is modeled in 3D using the KENO-V.a Monte Carlo code in the SCALE code system as shown in Fig. 3(b). The cask configuration is described in more detail in Refs. [6,13]. **Based on the previous descriptions, the GE10x10 lattice and the GBC-68 cask are the test models at which the two UQ approaches will be assessed**.

3.2. Data for computational UQ

The data for the computational approach features input parameters' uncertainty associated with the lattice design (i.e. GE10x10 lattice). Four main categories are considered within this type: (1) geometrical fuel data (e.g. pellet radius), (2) material data (e.g. U-235 enrichment), (3) operating conditions (e.g. coolant density), and (4) nuclear data (e.g. microscopic neutron cross-sections). The parametric uncertainty within these categories is obtained from different sources, mainly experimental analysis. Table 1 lists 1-σ uncertainty in relative form for various input parameters related to the prescribed categories along with the sources used to draw the data. It is worth mentioning that fuel design parameters such as pellet radius and U-235 enrichment are proprietary data for the fuel vendors and therefore difficult to obtain. According to Ref. [14], the uncertainties in fuel design parameters are based on prior experience and recommendations used in criticality safety analysis. The operating parameter uncertainties are based on previous benchmark reports [15,16], which reported that coolant density and fuel temperature uncertainties should be within 10% tolerance. We assume here that the tolerance value corresponds to 3-σ bound of a normal distribution. The last source is nuclear data uncertainties reported in nuclear data covariance libraries [17], where the measured uncertainty of the neutron cross-sections and other nuclear parameters is provided. In this study, we use the 56-group covariance library (56group-COV) in TRITON/T-DEPL depletion calculations as the source of nuclear data uncertainty. The uncertainties listed in Table 1 are used for random sampling of the input parameters in the computational approach.

3.3. Data for data-driven UQ

The data for the data-driven approach features radiochemical fuel assay data with nuclide concentrations of different isotopes that are measured based on a spent fuel rod discharged from a real reactor. A database developed by the OECD Nuclear Energy Agency called SFCOMPO contains measured nuclide data using different experimental techniques and for different reactor designs (e.g. PWR, BWR, CANDU). The latest version of SFCOMPO is reported in Ref. [20]. In this study, we focus on BWR measured data, since the test models (GE10x10, GBC-68) are based on BWR design.

Based on the previous section, the data-driven approach relies mainly on calculating the C/E ratio, which is then used to derive the uncertainty bounds for all isotopes in the inventory. In this paper, the C/E ratios are obtained from a thorough validation study performed over different BWR benchmarks using the SCALE code system [21] and the SFCOMPO database. It is worth mentioning that the validation process can be performed by the authors, but since the scope of the paper is on UQ methodology, and to ensure conciseness of the work, the validation results are obtained from an external source. In this external source, three selected benchmarks are considered: **8x8** Fukushima Daini-2, **7x7** Cooper, and **6x6** Gundremmingen units. By collecting all C/E values from the three benchmarks for the 10 actinides of interest, the bias mean ($\overline{R}_n$), standard deviation (σ_{R_n}), and the number of experimental samples (N_n) used to calculate such statistics are listed in Table 2. Since the objective in this paper is to validate and highlight two UQ approaches to propagate the isotopic uncertainty, a small data ensemble is used. However, to obtain more realistic uncertainty bounds, a large number of experimental samples should be considered. Also, it is worth mentioning that the 6x6 benchmark did not report measured data for U-234 and Am-241, which justifies the lower number of samples for these two isotopes in Table 2.

4. Results and discussion

The results of this study are presented in two subsections. The first subsection includes the results obtained from UQ of depletion calculations in both computational and data-driven approaches. Criticality safety UQ is presented in the second subsection; which presents how the depletion uncertainty is propagated into the cask k_{eff}.

4.1. Depletion UQ

The first step in the computational approach includes propagating the input uncertainties in Table 1 through TRITON/T-DEPL depletion calculations. The nominal concentration of the GE10x10 is determined by depleting the lattice in constant specific power of 25 kW/kg for about 1200 days, which yields a discharge burnup of ~30 GWD/MTU. As mentioned before, we have two main fuel types in the GE-10x10 lattice, UO_2 and gadolinium pins, see Fig. 3(a), which we expect to have uncertainty in their isotopic inventory at the end of cycle. By post-processing the isotopic concentration samples, a mean vector and covariance matrix ($\overline{\mathbf{C}}$, $\mathbf{\Sigma_C}$) can be determined for each fuel type, which can be used later for criticality safety UQ. Therefore, in the actual analysis, each fuel type is sampled according to its mean vector and covariance matrix.

The correlation matrix between the 10 actinides is shown in Fig. 4 for the UO_2 pin. Since both UO_2 and gadolinium correlation matrices look very similar, only the UO_2 correlation matrix is shown here for brevity. The effect of correlation on cask k_{eff} uncertainty is investigated by performing sampling from joint and marginal distributions as will be described in the next subsection. Therefore, forward criticality calculations in KENO-V.a are repeated for two cases, each case has 500 forward samples, where the samples are uncorrelated for the first case, and correlated for the second.

The correlation matrix shows that plutonium isotopes have strong positive correlation with each other, especially Pu-240, Pu-241, and Pu-242. The uranium isotopes have weak correlation between each other, and some negative correlation with specific

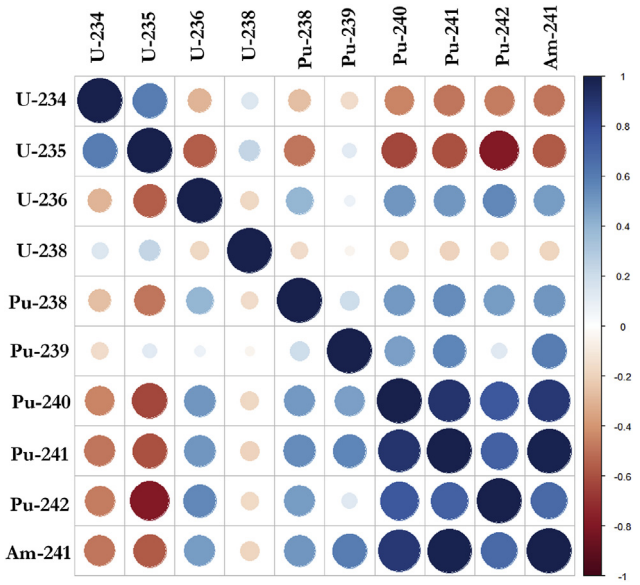

Fig. 4. Correlation coefficients between the major actinides for UO_2 pins after performing depletion calculations according to the computational approach.

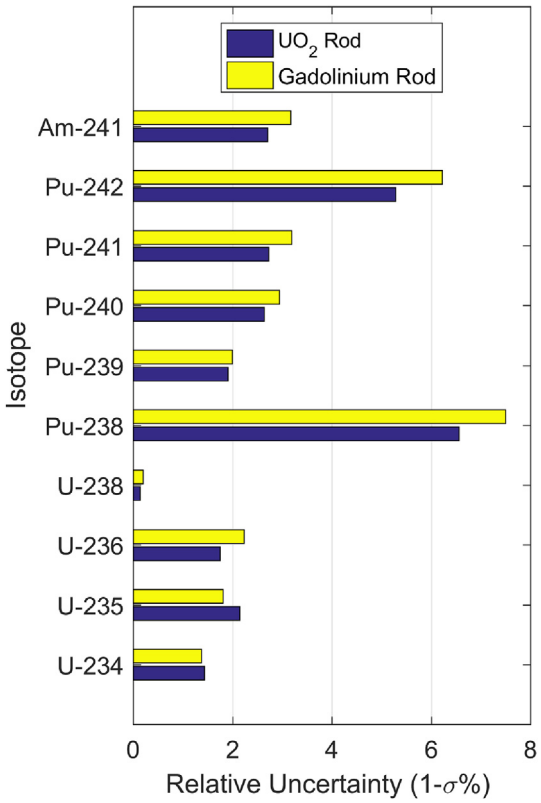

Fig. 5. The relative 1-σ uncertainty (in %) for major actinides after depletion analysis for UO_2 and gadolinium pins (by the computational approach).

plutonium isotopes. Am-241 shows mixed correlation between negative (e.g. with U-235), positive (e.g. Pu-241), and negligible (e.g. U-238). These conclusions hold true for the correlations in the gadolinium pins as well. Correlation between the heavy actinides is expected. For example, Pu-241 is generated by neutron capture in Pu-240, and Am-241 is mainly generated by beta decay of Pu-241. Since we assume that input parameters associated with geometry, operating conditions, and material are not correlated, the correlation in Fig. 4 is expected to arise from nuclear data covariances in SCALE data libraries (e.g. cross-section, fission yield, etc.). The 1-σ uncertainty for the major actinides as estimated from depletion calculations is listed in Fig. 5 for both UO_2 and gadolinium pins. We can observe that U-238 has the lowest relative uncertainty across all actinides. Pu-238 has the highest uncertainty among all actinides considered. In addition, the uncertainties in the gadolinium pin's isotopes are slightly higher than their UO_2 counterparts.

As described before in Section 3.2, the depletion UQ results for the data-driven approach are obtained from external validation study [21], and the summary of uncertainty bounds is reported in Table 2 for all actinides. We can notice that U-238 has the smallest bias and bias uncertainty, while Am-241 has the lowest agreement with 8% relative difference to data and large uncertainty in its bias. Comparison of ranking between the two methods shows good agreement. The computational approach ranks Pu-238, Pu-242, and Am-241, in order, as the three most uncertain isotopes, while the ranking of the data-driven approach, in order, is Am-241, Pu-238, and Pu-242.

4.2. Criticality safety UQ

In this subsection, the results of uncertainty propagation of cask k_{eff} are presented based on the uncertainty information drawn from Table 2 for data-driven and Fig. 5 for the computational approach. Table 3 lists the final cask k_{eff} uncertainty using three different methods: (1) computational approach with uncorrelated isotopic inventory, (2) computational approach with correlated isotopic inventory (see Fig. 4), and (3) the data-driven approach. The following notes are important to mention regarding the results in Table 3:

- Nominal k_{eff} value corresponds to the unperturbed cask k_{eff}, which is calculated based on the nominal nuclide concentrations ($\boldsymbol{C}^0$).
- All criticality safety results in Table 3 are based on 500 samples. Fig. 6 shows the convergence of k_{eff} uncertainty with number of samples for the computational and data-driven approaches.
- The uncertainty in Table 3 includes only the isotopic uncertainty to isolate its effect. The effect of uncertainty in nuclear data, cask geometry, etc. on cask k_{eff} is not included here.
- The cask is assumed to be flooded with full-density water to model the worst-case scenario.

The results in Fig. 6 show that the data-driven approach yields about 900 pcm uncertainty in k_{eff} due to the isotopic inventory. The computational approach with uncorrelated samples has the lowest uncertainty among all methods of about 300 pcm. In addition, we can observe that including the correlation between nuclides in the computational approach increases the uncertainty by about 100 pcm. The large uncertainty for the data-driven approach could be justified by the large bias uncertainty (σ_{R_n}), especially for the influential isotopes. The cask k_{eff} is expected to be more sensitive to U-235 and Pu-239 concentrations as compared to other isotopes. The bias for these two isotopes as in Table 2 is ~5%, compared to

Table 3
Comparison of cask k_{eff} uncertainty results as calculated by different approaches.

Method	Nominal k_{eff}	$\overline{k_{eff}}$	$\sigma_{k_{eff}}$ (%)	$\sigma_{k_{eff}}$ (pcm)
Computational (Uncorrelated)	0.79747	0.79762	0.39	314
Computational (Correlated)	0.79747	0.79812	0.50	403
Data-driven	0.79747	0.79762	1.11	888

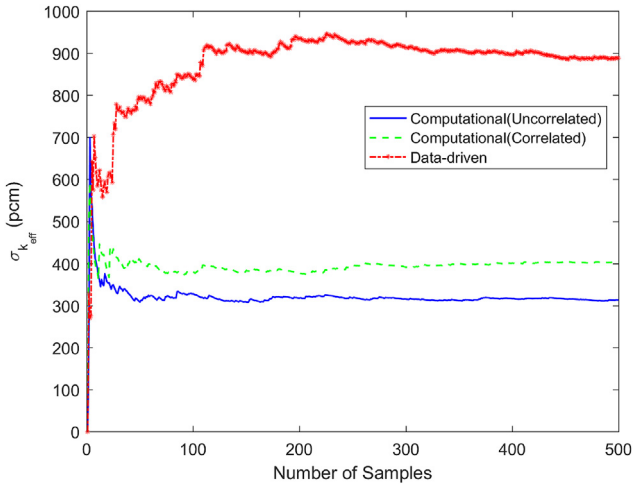

Fig. 6. Convergence of cask k_{eff} uncertainty as a function of number of samples for various methods.

their ~2% uncertainty in the computational approach (see Fig. 5). For the computational approach, although the uncertainty obtained here is below 500 pcm, this value relies significantly on the assigned input uncertainties in Table 1, especially those that are not associated with nuclear data libraries (e.g. operating data, geometry). Therefore, having an uncertainty library for the major input parameters in depletion calculations can be very helpful to characterize the uncertainty in the isotopic inventory by the computational approach.

From computational point of view, the computational approach is more expensive than the data-driven approach in this paper, since N_b forward depletion calculations are needed (500 in this study). For the data-driven approach, the number of depletion calculations equals to the experimental samples simulated to derive the bias information, C/E (32 in this study) plus one calculation for the nominal concentrations. However, the data-driven approach can be more expensive if large number of experimental samples are available (e.g. > 500), but their depletion models could be independent and have different cycle lengths.

Two gaps in this work can be observed. The first is that parametric uncertainty cannot be estimated by the data-driven approach. Doing so requires random sampling of the model parameters for each measured assay data, which will increase the computational cost of the data-driven approach significantly, as the sampling is performed over the expensive depletion calculations. The second assumption is that the data is assumed to be deterministic, as the measured uncertainty is not discussed in this work. In general, the reader can notice that the data-driven method can be easily modified to account for data uncertainty by treating each $R_n^{(i)}$ in Eq. (7) as a random distribution rather than a point-estimate. The denominator in Eq. (7) becomes a normal distribution represented by the measured concentration (mean) and its measured uncertainty (standard deviation). Afterward, the analyst needs to post-process $N_n \times n$ distributions to calculate the statistical estimators of the code bias in the data-driven approach.

Indeed, the previous two gaps inspire our next step for this work. It can be noticed that the computational approach is driven mainly by the "parametric" uncertainty of the depletion model, which is a single source. On the other hand, the data-driven approach relies on quantifying the model bias or discrepancy using real data. This type of uncertainty is also known as "predictive" or "model-form" uncertainty if different models with different forms are used [22]. Clearly, the predictive uncertainty seems to be more significant in this study compared to the parametric uncertainty. An idea can be tested on combining the two approaches into one hybrid approach using the Bayesian framework. In this hybrid approach, all uncertainty types, including data and parametric uncertainties, can be propagated in a flexible form similar to the study performed by Radaideh et al. [22] on nuclear thermal-hydraulics models.

5. Conclusions

We present two approaches for uncertainty propagation of the nuclide/isotopic composition into the criticality calculations of spent fuel casks. The first approach involves propagating input parameters' uncertainties into depletion calculations, which cause uncertainty in the isotopic composition. Parametric uncertainties include those associated with nuclear data, fuel geometry, material composition, and plant operation, where these uncertainties are based on experimental and prior experience in criticality safety. The second approach is data-driven which uses the measured radiochemcial assay data of nuclides to derive bias information (C/E). The bias is then sampled for each isotope and then the perturbed isotopic inventory from each approach can be propagated into the cask k_{eff}. We use measured data from the SFCOMPO database for three different BWR benchmarks: 6x6, 7x7, and 8x8. We apply the two UQ approaches on a BWR GE10x10 lattice and GBC-68 spent fuel cask for demonstration. The results show that the data-driven approach results in about 900 pcm uncertainty in cask k_{eff}, while the results for the computational approach uncertainty are lower. The correlation between the isotopes increases the uncertainty by the computational approach with about 100 pcm. The future work will include enhancing the databases with additional samples from the experiments available in SFCOMPO, and more parametric uncertainty bounds to make the uncertainty results more comprehensive. In addition, a hybrid approach of both computational and data-driven will be developed to propagate all uncertainty sources simultaneously using one method.

Declaration of competing interest

The authors have no conflict of interests to declare about this work.

Acknowledgements

This work is a part of the Cask Misload Evaluation Techniques project (16-10908) which is supported by U.S. Department of Energy (DOE) through Nuclear Energy University Programs (NEUP).

Appendix A. Supplementary data

Supplementary data to this article can be found online at https://doi.org/10.1016/j.net.2019.11.029.

References

[1] G. Radulescu, D.E. Mueller, J.C. Wagner, Sensitivity and uncertainty analysis of commercial reactor criticals for burnup credit, Nucl. Technol. 167 (2) (2009) 268–287.
[2] D. Rochman, A. Koning, D. Da Cruz, Propagation of ^{235,236,238}U and ^{239}Pu nuclear data uncertainties for a typical PWR fuel element, Nucl. Technol. 179 (3) (2012) 323–338.
[3] M. Pecchia, A. Vasiliev, H. Ferroukhi, A. Pautz, Criticality safety evaluation of a swiss wet storage pool using a global uncertainty analysis methodology, Ann. Nucl. Energy 83 (2015) 226–235.
[4] H.J. Park, D.H. Lee, B.K. Jeon, H.J. Shim, Monte Carlo burnup and its uncertainty propagation analyses for VERA depletion benchmarks by McCARD, Nucl. Eng. Technol. 50 (7) (2018) 1043–1050.
[5] W.A. Metwally, A.S. Alawad, B.A. Khuwaileh, On the over-conservatism of the

5% depletion uncertainty rule in spent fuel criticality analyses, Ann. Nucl. Energy 125 (2019) 1–11.
[6] M.I. Radaideh, D. Price, T. Kozlowski, Criticality and uncertainty assessment of assembly misloading in BWR transportation cask, Ann. Nucl. Energy 113 (2018) 1–14.
[7] A. Papoulis, S.U. Pillai, Probability, Random Variables, and Stochastic Processes, Tata McGraw-Hill Education, 2002.
[8] I. Gauld, Strategies for application of isotopic uncertainties in burnup credit, in: Tech. rep., NUREG/CR-6811, ORNL/TM-2001/257, US Nuclear Regulatory Commission, Oak Ridge National Laboratory, United States, 2003.
[9] H. Yun, K. Park, W. Choi, S.G. Hong, An efficient evaluation of depletion uncertainty for a GBC-32 dry storage cask with PLUS7 fuel assemblies using the Monte Carlo uncertainty sampling method, Ann. Nucl. Energy 110 (2017) 679–691.
[10] D. Price, M.I. Radaideh, D. O'Grady, T. Kozlowski, Advanced bwr criticality safety part ii: cask criticality, burnup credit, sensitivity, and uncertainty analyses, Prog. Nucl. Energy 115 (2019) 126–139.
[11] M.I. Radaideh, D. Price, D. O'Grady, T. Kozlowski, Advanced BWR criticality safety part I: model development, model validation, and depletion with uncertainty analysis, Prog. Nucl. Energy 113 (2019) 230–246.
[12] M.L. Fensin, Optimum Boiling Water Reactor Fuel Design Strategies to Enhance Reactor Shutdown by the Standby Liquid Control System, Master's thesis, University of Florida, 2004.
[13] D. Mueller, J. Scaglione, J. Wagner, S. Bowman, Computational benchmark for estimated reactivity margin from fission products and minor actinides in BWR burnup credit, in: Tech. rep., NUREG/CR-7157, ORNL/TM-2012/96, US Nuclear Regulatory Commission, Oak Ridge National Laboratory, United States, 2013.
[14] G. Ilas, H. Liljenfeldt, Decay heat uncertainty for BWR used fuel due to modeling and nuclear data uncertainties, Nucl. Eng. Des. 319 (2017) 176–184.
[15] G. M. Grandi, J. A. Borkowski, Benchmark of SIMULATE-3K against the frigg loop stability experiments, In: Proc. Advances in Nuclear Fuel Management III (ANFM 2003) Hilton Head Island, South Carolina, United States, October 5-8, 2003.
[16] M. Kruners, G. Grandi, M. Carlssonc, PWR transient xenon modeling and analysis using studsvik CMS, In: Proc. 2010 LWR Fuel Performance/TopFuel/WRFPM Orlando, Florida, United States, September 26-29, 2010.
[17] S.M. Bowman, Scale 6: comprehensive nuclear safety analysis code system, Nucl. Technol. 174 (2) (2011) 126–148.
[18] A. Hoefer, T. Ivanova, B. Rearden, D. Mennerdahl, O. Buss, Proposal for benchmark phase IV role of integral experiment covariance data for criticality safety validation, in: Tech. rep., Working Party on Nuclear Criticality Safety, OECD Nuclear Energy Agency, France, 2015.
[19] J.B. Briggs, L. Scott, A. Nouri, The international criticality safety benchmark evaluation project, Nucl. Sci. Eng. 145 (1) (2003) 1–10.
[20] F. Michel-Sendis, I. Gauld, J. Martinez, C. Alejano, M. Bossant, D. Boulanger, O. Cabellos, V. Chrapciak, J. Conde, I. Fast, et al., SFCOMPO-2.0: an OECD NEA database of spent nuclear fuel isotopic assays, reactor design specifications, and operating data, Ann. Nucl. Energy 110 (2017) 779–788.
[21] U. Mertyurek, M.W. Francis, I.C. Gauld, SCALE 5 analysis of BWR spent nuclear fuel isotopic compositions for safety studies, in: Tech. rep., ORNL/TM-2010/286, Oak Ridge National Laboratory, United States, 2010.
[22] M.I. Radaideh, K. Borowiec, T. Kozlowski, Integrated framework for model assessment and advanced uncertainty quantification of nuclear computer codes under bayesian statistics, Reliab. Eng. Syst. Saf. 189 (2019) 357–377.